

RESEARCH

Open Access



# Knockout IL4I1 affects macrophages to improve poor efficacy of CD19 CAR-T combined with PD-1 inhibitor in relapsed/refractory diffuse large B-cell lymphoma

Rui Zhang<sup>1</sup> , Yi Zhang<sup>2</sup>, Hairong Xiao<sup>3</sup>, Qingxi Liu<sup>3\*</sup> and Mingfeng Zhao<sup>1,2\*</sup>

## Abstract

Chimeric antigen receptor (CAR) T-cell therapy plays a critical role in the treatment of B-cell hematologic malignancies. The combination of PD-1 inhibitors and CAR-T has shown encouraging results in treating patients with relapsed/refractory (R/R) diffuse large B-cell lymphoma (DLBCL). However, there are still cases where treatment is ineffective. This study aimed to investigate the role of IL4I1 in the poor efficacy of CD19 CAR-T combined with PD-1 inhibitors in R/R DLBCL and to explore potential mechanisms. Transcriptomic and metabolomic correlation analyses were performed on tumor tissue from DLBCL patients. We employed an in vitro co-culture system consisting of Pfeiffer cells, CD19 CAR-T and macrophages to investigate the underlying mechanisms. It was found that IL4I1 levels were significantly increased in the tumor tissues of R/R DLBCL patients compared to responders. Correlation analysis revealed a positive association between IL4I1 and tryptophan (Trp)-kynurenic acid (Kyn) related metabolites. In the in vitro co-culture model, the presence of IL4I1 inhibited the cytotoxicity of CAR-T cells. Depletion of IL4I1 disrupted the IDO-AHR-Kyn signaling pathway, thereby enhancing the effectiveness of PD-1 inhibitors in combination with CD19 CAR-T for DLBCL treatment. CAR-T-mediated cytotoxicity was significantly inhibited when IL4I1 was present in the in vitro co-culture model. These findings suggest that IL4I1 may be a contributing factor to poor prognosis in R/R DLBCL patients. IL4I1 expression enhances immunosuppression via the IDO-AHR-Kyn pathway, inhibiting the effectiveness of PD-1 inhibitors combined with CD19 CAR-T. Therefore, suppression of IL4I1 may represent a potential target for combination therapy in DLBCL.

**Keywords** CD19 CAR-T, PD-1 inhibitor, DLBCL, IL4I1, Metabolism

\*Correspondence:

Qingxi Liu  
liuqingxi66@aliyun.com  
Mingfeng Zhao  
mingfengzhao@sina.com

<sup>1</sup>Department of Hematology, Tianjin First Central Hospital, Tianjin, China

<sup>2</sup>Department of Hematology, First Center Clinic College of Tianjin Medical University, Tianjin, China

<sup>3</sup>Boyalife wsn Ltd, Shen Zhen, China



© The Author(s) 2024. **Open Access** This article is licensed under a Creative Commons Attribution-NonCommercial-NoDerivatives 4.0 International License, which permits any non-commercial use, sharing, distribution and reproduction in any medium or format, as long as you give appropriate credit to the original author(s) and the source, provide a link to the Creative Commons licence, and indicate if you modified the licensed material. You do not have permission under this licence to share adapted material derived from this article or parts of it. The images or other third party material in this article are included in the article's Creative Commons licence, unless indicated otherwise in a credit line to the material. If material is not included in the article's Creative Commons licence and your intended use is not permitted by statutory regulation or exceeds the permitted use, you will need to obtain permission directly from the copyright holder. To view a copy of this licence, visit <http://creativecommons.org/licenses/by-nc-nd/4.0/>.

## Introduction

Diffuse large B-cell lymphoma (DLBCL) is a malignant and invasive tumor that accounts for 30–50% of non-Hodgkin lymphomas. The standard treatment for CD20-positive DLBCL is R-CHOP (rituximab in combination with cyclophosphamide, doxorubicin, vincristine, and prednisone) [1, 2]. However, approximately 30–40% of patients either do not respond or experience relapse. CD19 CAR-T therapy has demonstrated promising results in relapsed/refractory (R/R) DLBCL, yet there remains significant room for improvement.

CD19 CAR-T is an important treatment for R/R DLBCL, achieving a complete response (CR) rate of over 50% and an objective response rate (ORR) of approximately 70% [3, 4]. However, the efficacy of CD19 CAR-T therapy in R/R DLBCL may be compromised by factors such as the immunosuppressive tumor microenvironment (TME) [5]. Macrophages, which are abundant immune cells in the DLBCL microenvironment, play a critical role in CAR-T cell exhaustion and the inhibition of CAR-T cytotoxicity [6, 7]. Thus, further research is needed to optimize CAR-T therapy in DLBCL and overcome the challenges posed by the immunosuppressive TME. The strategy of combining CAR-T therapy with immune checkpoint inhibitors holds promise for enhancing the effectiveness of this treatment approach in R/R DLBCL patients.

Immune checkpoint inhibitors, such as PD-1/PD-L1 inhibitors, can help overcome immune suppression in the TME and enhance CAR-T cell activity [8, 9]. The use of PD-1 inhibitors in combination with CAR-T therapy has shown promise in preclinical models and clinical trials [10, 11]. Our previous research found that combining immune checkpoint inhibitors to block PD-1 can enhance CAR-T cell efficacy in R/R DLBCL [12]. This combination approach has been particularly effective in treating R/R DLBCL patients with TP53 mutations or deletions who were unresponsive to CAR-T cell therapy [13]. However, it is important to note that cases of treatment failure have occurred in R/R DLBCL patients treated with PD-1 inhibitors in combination with CAR-T therapy [14]. For instance, a prospective study reported a relatively low ORR of 25% with pembrolizumab following CD19 CAR-T therapy in non-Hodgkin lymphoma (NHL) [15]. While the combination of CAR-T and PD-1 inhibitors holds promise, these findings highlight the need for further research to identify factors contributing to treatment failures and to optimize the timing, dosing, and patient selection for combination therapy. A comprehensive understanding of the underlying mechanisms and careful patient selection will be crucial for improving the outcomes of combination therapies in R/R DLBCL.

Single-cell sequencing data reveal that IL4I1, PD-L1, and IDO1 are expressed in macrophages clustering

around tumors in a T cell-dependent manner [16]. IL4I1 functions as an amino acid oxidase that activates the aryl hydrocarbon receptor (AhR) by recognizing tryptophan (Trp) and generating metabolites such as indole and uric acid [17]. Reduced expression of IL4I1 has been shown to inhibit the conversion of certain amino acids to acetyl-coenzyme A, affecting energy metabolism pathways, and has been correlated with reversing resistance to the drug ibrutinib in DLBCL [18]. This suggests that targeting IL4I1 may have therapeutic potential in combating drug resistance in DLBCL. Furthermore, PD-1 signaling on T cells has been found to inhibit metabolic pathways associated with T cell activation [19]. This underscores the importance of metabolic modulation in conjunction with PD-1 blockade to improve CAR-T therapy effectiveness. The combination of metabolic inhibitors and PD-1 inhibitors may enhance therapeutic outcomes in DLBCL. Based on these findings, it is suggested that suppressing IL4I1 expression can reverse resistance to PD-1 inhibitors in combination with CAR-T therapy, further emphasizing IL4I1 as a potential therapeutic target to enhance the efficacy of combination therapies in DLBCL.

## Materials and methods

### Cell culture and isolation of primary cells

HEK-293T and Pfeiffer cells were purchased from the American Type Culture Collection (ATCC, Manassas, VA, USA). HEK-293T cells were cultured in DMEM (Gibco) supplemented with 10% FCS (Gibco), while Pfeiffer cells were cultured in RPMI 1640 supplemented with 10% FCS. Peripheral blood mononuclear cells (PBMCs) from healthy individuals and lymphoma tissues from relapsed/refractory (R/R) patients and responders who received a PD-1 inhibitor in combination with CD19 CAR-T were collected at Tianjin First Central Hospital. Healthy donors and lymphoma patients consented to participate in this experiment as part of a clinical trial (ChiCTR-ONN-16009862; Medical Ethics Committee of the First Central Hospital of Tianjin). The FMC63 clone served as the source of the scFv plasmid targeting CD19. The scFv, human 4-1BB, and CD3 $\zeta$  signaling domains of the CAR vectors were subcloned into the lentiviral plasmid pCDHMND-MCS-T2A-Puro. The RQR8 tag was placed in front of the CAR sequence, with a short T2A peptide in between for identification. Ethical approval and informed consent were obtained from the Tianjin First Central Hospital Medical Ethics Committee (Tianjin, China) for all human samples used in this study, which were approved under clinical trial No. ChiCTR-ONN-16,009,862. All methods were performed in accordance with relevant guidelines and regulations.

### Plasmids, siRNA, and cell transfection

We utilized the CRISPR-Cas9 technique to knock down IL4I1 in M-THP1 cells and selected three gRNA sequences: GGGTAGAAAATCATGCGCGA; GCTG GCCTCGTACACGTGGT; GCACCGGCGTCGTCA AGCGT. MyBiosource provided a human IL4I1 cDNA clone with Gateway-compatible recombination sites (MBS1270935). According to the manufacturer's instructions (GeneCopoeia, Rockville, MD, USA), lentivirus was prepared for transfection experiments. After 6 h of incubation, the medium was replaced with DMEM-F12 supplemented with 10% FBS. Transfection was performed following the manufacturer's instructions. Subsequently, PCR, Western blot, and luciferase analysis assays were conducted as described below.

### Lentivirus production

Lentivirus was prepared according to the manufacturer's instructions (GeneCopoeia). For HEK-293T lentiviral packaging cells, it is recommended to culture them in DMEM supplemented with 10% heat-inactivated fetal bovine serum and to perform transfection when the cells reach 70–80% confluence. Dilute 2.5 µg of the lentiviral expression plasmid and 2.5 µg of Lenti-Pac HIV mix in 200 µL of Opti-MEM® I (Invitrogen). For separate tube preparation, combine 15 µL of EndoFectin Lenti with 200 µL of Opti-MEM I and mix by adding dropwise to the plasmid mixture, followed by a 10–25 min incubation at room temperature. After transfection, the culture medium containing pseudovirus was collected after 48 h, and ultracentrifugation was performed. The pellets were then resuspended in complete X-Vivo15 medium and stored at –80 °C for later use.

### Production and detection of CAR-T cells

CD3<sup>+</sup> T cells from healthy donors were isolated from PBMCs using CD3 immunomagnetic beads (Miltenyi Biotec, Germany; #130-097-043) and subsequently stimulated with CD3/CD28 beads (Thermo Fisher Scientific; #11131D) and IL-2 (100 IU/mL; Miltenyi Biotec) in X-VIVO 15 medium (Lonza). Following activation and expansion for 48 h, cells were transduced with lentivirus two hours later. To express a CD19-specific CAR, T cells were typically engineered for 9–12 days and then stained with Alexa-Fluor 647-labeled polyclonal goat anti-mouse IgG (H+L) antibodies (Affinity). Additionally, all cells were further confirmed by staining with fluorescein isothiocyanate (FITC)-labeled anti-CD3 antibodies (Abcam).

### Cell co-culture model

THP1 cells ( $5 \times 10^5$ /well) were seeded into six-well plates and polarized into M2 macrophages by treating them with 320 nM PMA (Sigma) for 24 h, followed by

the addition of 20 ng/mL IL-4 (PeproTech) and 20 ng/mL IL-13 (PeproTech) in the presence of PMA for an additional 24 h to obtain the M2 phenotype. Flow cytometry was used to validate the formation of M2 macrophages based on the surface markers CD11b and CD163. Following a wash to remove all PMA and cytokines, a co-culture of  $2 \times 10^5$  M2 macrophages (IL4I1 KO or control),  $2 \times 10^5$  CAR-T cells, and  $6 \times 10^5$  Pfeiffer cells was incubated in X-VIVO 15 medium (Lonza) supplemented with IL-2 (100 IU/mL, Miltenyi Biotec) for 24–48 h.

### Immunocytochemistry assay

After treatment, cells were fixed with 4% paraformaldehyde for 20 min and subsequently blocked with normal goat serum at room temperature for 30 min. Following overnight incubation with rabbit anti-AhR (Abcam) in a humid chamber, cells were then incubated with FITC-conjugated goat anti-rabbit IgG (Santa Cruz) for 30 min at 37 °C. After washing with PBS, samples were examined using a confocal laser scanning microscope. DAPI staining (blue) was used to visualize total nuclei. Immunohistochemical staining was performed to analyze tumor tissue according to the established protocol. After deparaffinization and rehydration, sections were exposed to 3% H<sub>2</sub>O<sub>2</sub> in methanol and then blocked with 1% BSA for 30 min at room temperature. After blocking, sections were incubated overnight at 4 °C with anti-IL4I1 primary antibodies and subsequently with peroxidase-conjugated secondary antibodies. The number of IL4I1<sup>+</sup> cells was determined by counting stained cells.

### Quantitative real-time PCR (qRT-PCR)

Real-time PCR (Biosystems StepOne, Foster City, CA, USA, Applied Biosystems) was used to measure the mRNA levels of specific genes using Fast SYBR Green Master Mix (Applied Biosystems, Waltham, MA, USA). The thermocycling conditions included denaturation at 95 °C for 30 s, followed by 45 s of annealing at temperatures ranging from 48 °C to 70 °C, and a final extension step of 30 s at 72 °C for 30–32 cycles. The mean of three independent experiments performed in triplicate is represented by the error bars, with one standard error of measurement. The following primers were used: IL4I1 forward 5'CGCCCGAAGAC ATCTACCAG3', reverse 5'GATATTCCAAGAGCGTGTGCC3'.

### Metabolomics sequencing

Metabolomics sequencing was performed using a methanol-based extraction method to extract intracellular metabolites from each biological replicate. Prior to extraction, cells were harvested, counted, and divided into three aliquots. The cells were washed with cold PBS before the addition of 250 µL of LC-MS grade methanol. The resulting mixture was then pelleted, and 150 µL of

the supernatant was transferred to an LC-MS vial. After obtaining the metabolite data, cluster analysis was performed to identify patterns and similarities among the selected differential metabolites. Additionally, metabolite correlation analysis was conducted to explore the relationships between different metabolites within the two groups.

#### Cytotoxicity against Pfeiffer in vitro

For this experiment,  $4 \times 10^5$  CD19 CAR-T cells per group were seeded in a co-culture with Pfeiffer cells and M-THP1 in a ratio of 1:3:1 and incubated for 48 h. The experiment included 36  $\mu\text{g}/\text{mL}$  of a PD-1 inhibitor (Bristol-Myers Squibb, New York, NY, USA) and was designed to evaluate CAR-T cell killing of Pfeiffer cells. Cytotoxicity was determined using a lactate dehydrogenase (LDH) assay kit (Dojindo Molecular Technologies, Inc.) and monitored at 0, 24, and 48 h after cell co-culture. Isolation of CD19 CAR-T cells from the co-culture was achieved by MACS using CD3 microspheres as previously described. An LDH cytotoxicity assay kit (Dojindo Molecular Technologies, Inc.) was used to detect cytotoxicity at 490 nm at 0, 24, and 48 h.

#### Western blotting and cytokine release analysis

Western immunoblotting was performed according to previously described methods [20]. After SDS-PAGE and blotting, proteins were detected using the following primary antibodies: IDO (Bioss, bs-15493R), Kyn (Abcam, ab276053), and mouse anti-GAPDH (Santa Cruz). The secondary antibodies used were IRDye-800-conjugated anti-mouse and anti-rabbit immunoglobulin G (Li-COR Biosciences) at a dilution of 1:200. Immunofluorescence was performed using the Odyssey infrared imaging system from Gene Company Ltd. GAPDH expression was used as an internal control.

#### Evaluation of CAR-T cells' efficacy and adverse effects in B-Cell lymphoma mouse xenograft models

Male NSG mice aged 6–8 weeks were chosen for the establishment of B-cell lymphoma mouse xenograft models. The mice were injected with  $5 \times 10^6$  Pfeiffer cells expressing luciferase by subcutaneous injection on one side. Established tumors were monitored by bioluminescence imaging (BLI). Upon confirmation of engraftment after 20 days, the mice were randomized into three groups and treated by tail vein injection of  $5 \times 10^6$  CD19 CAR-T cells and  $2.5 \times 10^6$  M-THP1. During treatment, we assessed tumor burden by employing the IVIS Lumina II (PerkinElmer) imaging system following intraperitoneal administration of 3 mg of D-fluorescein (Sigma) to each mouse at predetermined time intervals. The Animal Care and Use Committee of Tianjin Medical University approved the animal experimental protocol.

#### Statistical analysis

Statistical analysis was performed using SPSS 17.0 (SPSS, Inc., Chicago, IL, USA). Data are expressed as the mean  $\pm$  standard error and analyzed using a *t*-test, with the *q*-test method used for pairwise comparison. A *p*-value of  $< 0.05$  was considered statistically significant.

#### Results

##### IL4I1 as a factor for poor prognosis in DLBCL patients

High expression of IL4I1 in tumor-associated macrophages (TAMs) may contribute to drug resistance and poor prognosis in DLBCL patients. IL4I1 is known to promote tumor cell proliferation and suppress immune responses [18]. Therefore, we hypothesized that elevated IL4I1 expression could be associated with drug resistance and poor prognosis in DLBCL patients. To test this hypothesis, we analyzed the mRNA levels of IL4I1 in PBMCs of healthy individuals, as well as in initial lymphoma tissue from patients with relapsed/refractory (R/R) DLBCL who responded to combination therapy (Fig. 1A). The results showed that IL4I1 mRNA levels in the tumor tissue of R/R patients were significantly higher than those in PBMCs of healthy individuals ( $P < 0.001$ ). However, there was no statistically significant difference in IL4I1 mRNA levels between responders and healthy individuals. These findings suggest that IL4I1 may contribute to the unfavorable prognosis of DLBCL patients. Immunohistochemistry analysis of tumor tissue revealed significantly higher expression of IL4I1 in the R/R group compared to the response group (Fig. 1B). Based on immunohistochemical analysis of IL4I1 in tumor tissue, the number of positive cells (brownish-yellow staining) ranged from 70 to 100% in the R/R group, while it ranged from 0 to 10% in the response group, indicating that IL4I1 adversely affects patient prognosis (Fig. 1B). Thus, IL4I1 may be a contributing factor to the unfavorable prognosis of these patients.

For transcriptomic and metabolomic correlation analyses, three samples were randomly selected from R/R and responder patients. Group 1 was defined as R/R patients after combination therapy, while Group 2 comprised patients who achieved a response after combination therapy. The volcano plot offers a visual representation of the differential metabolic pathways distribution between the two groups. The horizontal axis denotes the expression change of proteins associated with metabolic pathways between the two groups ( $\log_2$  Fold Change), while the vertical axis reflects the significance level of proteins differences ( $-\log_{10}$  *p*value). Up-regulated genes are depicted as red dots, whereas down-regulated genes are represented by green dots. Approximately 165 proteins associated with metabolic pathways exhibited differential expression between the two groups, of which about 89 proteins were up-regulated and 76 proteins



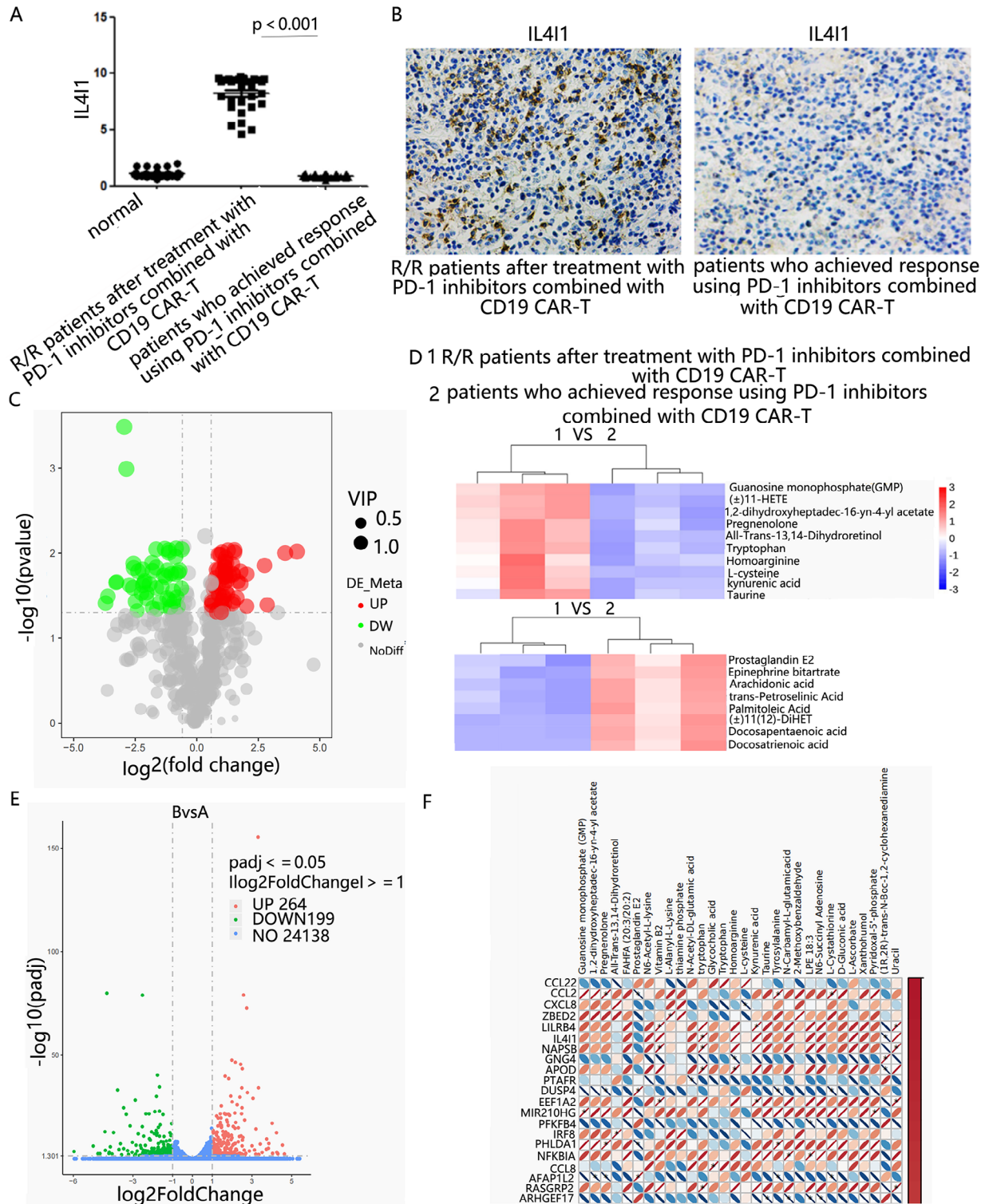


**Fig. 1** IL411 as a Factor for Poor Prognosis in DLBCL Patients. The groups are divided into Group 1 and Group 2. Group 1: R/R patients after treatment with a PD-1 inhibitor in combination with CD19 CAR-T; Group 2: Patients with a response after treatment with a PD-1 inhibitor in combination with CD19 CAR-T. (A) The mRNA levels of IL411 in different groups. (B) Immunohistochemical analysis of IL411 in lymphoma tissue across different groups. (C) The volcano plot offers a visual representation of the differential metabolic pathways distribution between the two groups. (D) The heatmap illustrates several metabolic pathways between the two groups. (E) The volcano plot displays differentially expressed genes between the two groups combination with 463 out of 24,601 metabolic pathways showing significant differences. (F) Proposed interaction map of transcriptomic and metabolomic data regulated by IL411

were down-regulated in the group that did not respond to combination therapy (Fig. 1C). The heatmap illustrates several proteins associated with metabolic pathways between the two groups. We found that kynurenic acid (Kyn), tryptophan (Trp), and tyrosylalanine were significantly upregulated in Group 1 compared to Group 2, whereas arachidonic acid (AA) and prostaglandin E2 (PGE2) were downregulated (Fig. 1D). More than 20,000 differentially expressed genes are displayed in the volcano plot. The horizontal axis denotes the expression change of differentially genes between the two groups (log<sub>2</sub> Fold Change), while the vertical axis reflects the significance level of genes differences (-log<sub>10</sub> pvalue). Up-regulated genes are about 264, whereas down-regulated genes are about 199 (Fig. 1E). Transcriptomic and metabolomic correlation analysis showed that IL4I1 was significantly positively correlated with Kyn and Trp-related metabolites (Fig. 1F).

#### **Effect of IL4I1 on CD19 CAR-T and PD-1 inhibitor combination therapy**

To assess the impact of IL4I1 on the efficacy of PD-1 inhibitors in combination with CD19 CAR-T treatment, an improved in vitro co-culture model was employed to simulate the tumor microenvironment. The co-culture system consisted of CD19 CAR-T cells, Pfeiffer cells, and M-THP1 cells (IL4I1 KO or control) in a specific ratio of 1:3:1. The cytotoxicity of CAR-T cells against Pfeiffer cells was measured using lactate dehydrogenase (LDH) activity. As shown in Figs. 2A and 38.73% of Pfeiffer cells were killed after being exposed to CD19 CAR-T combined with PD-1 inhibitor for 24 h, and 92.27% were killed at 48 h. After transfecting IL4I1 overexpression plasmid into the M-THP1 cells, the cytotoxicity of CD19 CAR-T combined with PD-1 inhibitor were significantly inhibited, only about 47.8% of Pfeiffer cells were killed at 48 h. Moreover, IL4I1 KO in the M-THP1 cells, the cytotoxicity of CD19 CAR-T combined with PD-1 inhibitor were significantly increased (Fig. 2B). Subsequently, we evaluated the subtype of the IL4I1 knockout (IL4I1 KO) group and the control group, revealing a balanced proportion of CD4-positive and CD8-positive CAR-T cells at approximately 50% each (Fig. 2C). Meanwhile, cellular differentiation detection was conducted to analyse the proportion of effective and memorable subtypes. The result showed that the IL4I1 KO group had a higher proportion of Naïve T cells in CD4 or CD8 positive CD19 CAR-T cells compared to the control group (Fig. 2D). Additionally, the expression levels of immune checkpoint markers PD-1, TIM-3, and LAG-3 on CD19 CAR-T cells were comparable between the IL4I1 KO and control groups. However, the IL4I1 KO group exhibited a lower proportion of CD19 CAR-T cells expressing PD-1, TIM-3, and LAG-3 than control groups (Fig. 2E). Quantification from

three independent experiments is presented in Fig. 2F. These findings suggest that IL4I1 plays a significant role in influencing the effectiveness of CD19 CAR-T therapy in combination with PD-1 inhibitors.

#### **IL4I1 enhances immune suppression via the IDO1-AHR-Kyn metabolic pathway**

Indoleamine 2,3-dioxygenase (IDO1) has been implicated in promoting the proliferation of malignant cells in gliomas and is associated with poor prognosis [21]. In the co-culture system of CAR-T cells, Pfeiffer cells, and M-THP1 cells, the expression of IDO1 increased, while knockout of IL4I1 in M-THP1 cells inhibited IDO1 expression (Fig. 3A). IL4I1 knockout in M-THP1 cells significantly reduced IDO1 expression in CD19 CAR-T/CD19 CAR-T combined with PD-1 inhibitor treatment, while IL4I1 overexpression in M-THP1 cells increased IDO1 expression (Fig. 3B, C). These findings suggest that IL4I1 may enhance the expression of immunosuppressive proteins in macrophages, potentially impairing the efficacy of CAR-T therapy.

Based on previous studies, we hypothesized that an IDO inhibitor could inhibit the Trp-Kyn pathway in the DLBCL microenvironment. In the in vitro co-culture model, the IDO inhibitor partially blocked the Trp-Kyn pathway in CD19 CAR-T/CD19 CAR-T combined with PD-1 inhibitor treatment, as demonstrated by western blot analysis (Fig. 3D-E). Immunofluorescence detection showed that the fluorescence intensity of the aryl hydrocarbon receptor (AhR) in the IDO inhibitor group (CD19 CAR-T combined with PD-1 inhibitor treatment and added IDO inhibitors) was lower than that in the control group (CD19 CAR-T combined with PD-1 inhibitor treatment) (Fig. 3F). These results indicate that even with the addition of a PD-1 inhibitor, IDO1 continues to drive the Trp-Kyn pathway. The combination of PD-1 inhibitors and IDO inhibitors to reduce Kyn AhR expression was effective. IL4I1 KO in M-THP1 cells in the co-culture system significantly inhibited Kyn expression in CD19 CAR-T/CD19 CAR-T combined with PD-1 inhibitor treatment (Fig. 3G, H). Immunofluorescence detection showed that AhR fluorescence intensity in the IL4I1 KO group was lower than that in the control group (Fig. 3I). These results suggest that the presence of IL4I1 may enhance the expression of immunosuppressive proteins in macrophages, while the efficacy of CAR-T therapy may be increased by IL4I1 KO in macrophages.

#### **IL4I1 inhibition in macrophages increases CAR-T treatment in vivo**

In a xenograft mouse model, M2 macrophages exerted a strong inhibitory effect on CD19 CAR-T therapy, which was reversed by the knockout of IL4I1. To further evaluate the impact of IL4I1 on CAR-T therapy and its

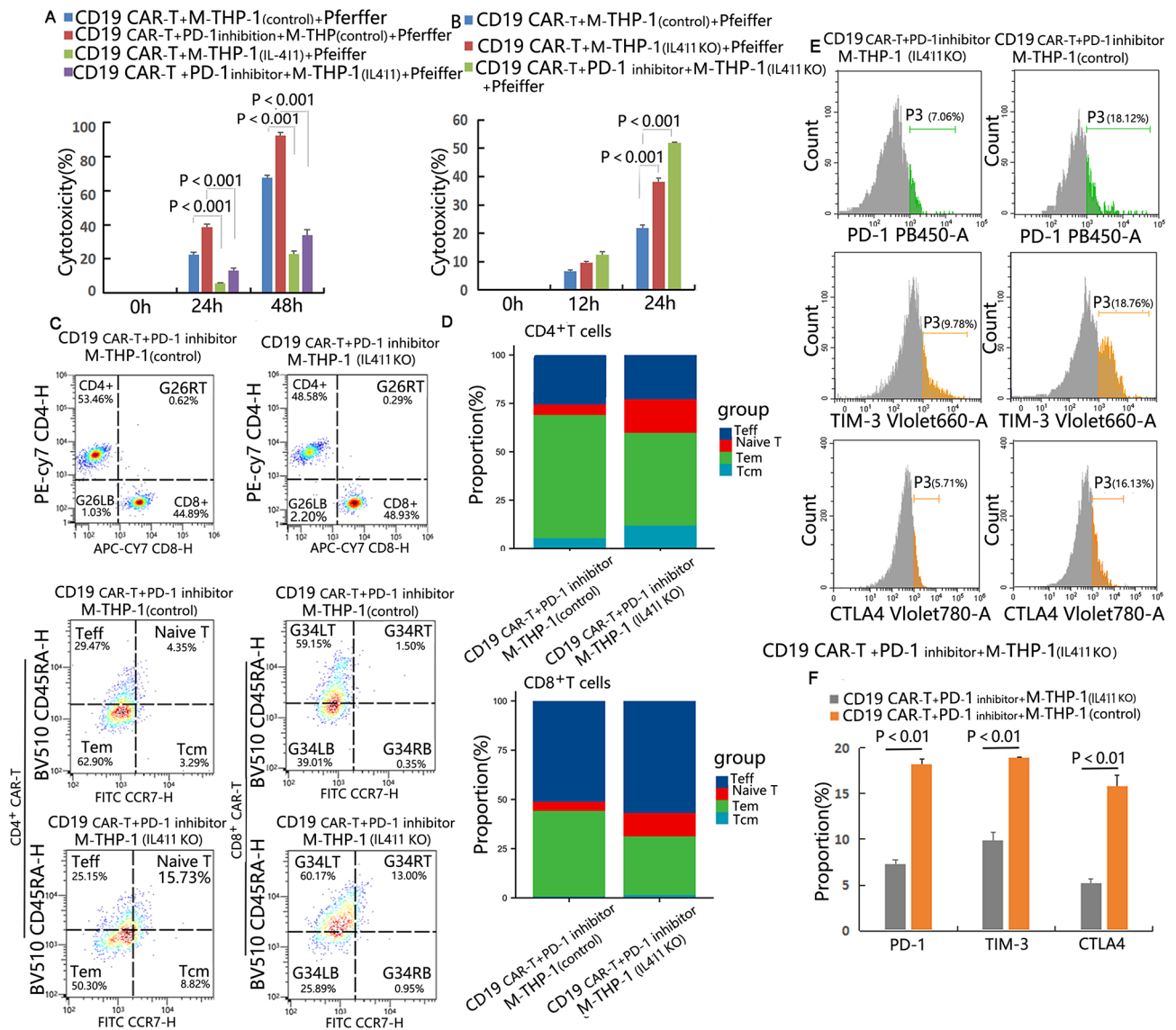


**Fig. 2** Effect of IL411 on CD19 CAR-T and PD-1 Inhibitor Combination Therapy. The in vitro co-culture model consisted of CAR-T cells, Pfeiffer cells, and M-THP1/M-THP1 (IL411 KO)/M-THP1 (IL411 overexpression) in a ratio of 1:3:1, with 36  $\mu\text{g}/\text{mL}$  of PD-1 inhibitor added. After 24 h (or 48 h for cytotoxicity) of incubation, the following analyses were conducted: **(A)** Impact of IL411 overexpression on cytotoxicity; **(B)** Impact of IL411 knockout on cytotoxicity; **(C)** CD4/CD8 ratio and subtype analysis in the IL411 KO group and control group; **(D)** Quantification of the CD4/CD8 ratio and subtype analysis; **(E)** Proportion of CAR-T cells expressing PD-1, TIM-3, and LAG-3; **(F)** Quantification of the expression of PD-1, TIM-3, and LAG-3 on CAR-T cells

function, a xenograft model was utilized. After confirming tumor engraftment, the mice were randomized into three groups and treated with a tail vein injection of  $5 \times 10^6$  CD19 CAR-T cells and  $2.5 \times 10^6$  M-THP1 cells. As shown in Fig. 4A, the combination of CD19 CAR-T treatment, IL411 KO M-THP1 cells, and a PD-1 inhibitor resulted in a significant therapeutic effect, with almost complete eradication of tumors by day 35. In contrast, the group treated with control M-THP1 cells displayed continuous tumor growth and spread.

The presence of CD19 CAR-T cells in the bone marrow (BM) was also quantified, and the results showed that the CD19 CAR-T cells combined with IL411 KO M-THP1

cells and the PD-1 inhibitor exhibited sustained proliferation from day 7 to day 28, consistent with the observed tumor elimination (Fig. 4B). Survival analysis demonstrated that mice treated with CD19 CAR-T cells, IL411 KO M-THP1 cells, and a PD-1 inhibitor had the longest survival time, with no deaths recorded (Fig. 4C).

## Discussion

There are many possible factors for the poor efficacy of CAR-T cell therapy on R/R DLBCL, among which immunosuppressive tumor microenvironment is an important factor [5]. Strategies to enhance CAR-T cell efficacy encompass modifications of CAR-T components [22], the

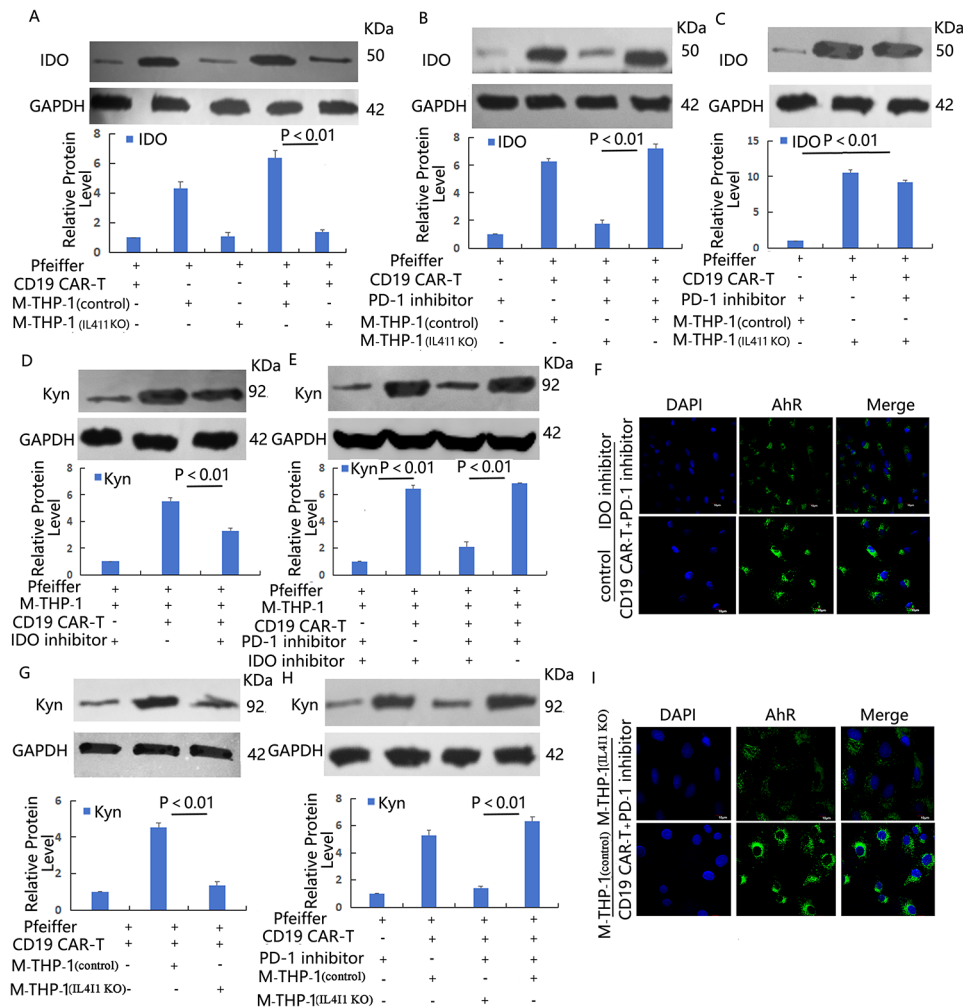


**Fig. 3** IL411 Enhances Immune Suppression via the IDO1-AHR-Kyn Metabolic Pathway. The in vitro co-culture model consisted of CAR-T cells, Pfeiffer cells, and M-THP1/M-THP1 (IL411 KO)/M-THP1 (IL411 overexpression) in a ratio of 1:3:1, with the addition of 5 mM IDO inhibitor D-1MT and 36  $\mu$ g/mL PD-1 inhibitor. After 24 h (or 48 h for cytotoxicity) of incubation, the following analyses were conducted: **(A-C)** Protein expression of IDO1 in cell lysates was analyzed by western blot; **(D-E)** Protein expression of kynurenine (Kyn) treated with the IDO inhibitor in the co-culture model; **(F)** Immunofluorescence detection of Kyn treated with the IDO inhibitor and PD-1 inhibitor in the co-culture model; **(G-H)** Protein expression of Kyn in cell lysates analyzed by western blot in the co-culture model; **(I)** Immunofluorescence detection of Kyn treated with the IDO inhibitor and PD-1 inhibitor in the co-culture model

incorporation of novel targets or multi-target sites [23], and combination therapies with additional drugs [24]. Currently, combining immune checkpoint inhibitors represents a promising therapeutic approach [25]. Our clinical trials have revealed that CD19 CAR-T therapy has the potential to be more effective in treating relapsed/refractory (R/R) DLBCL patients with high tumor burden when combined with a PD-1 inhibitor [12]. However, the tumor microenvironment (TME) in R/R DLBCL has also contributed to the failure of combination therapy in some cases [14]. Therefore, further research into additional mechanisms of TME regulation is essential to combat drug resistance.

PD-1 inhibitors have the potential to improve CAR-T function by downregulating PD-1 expression on T cells [12, 26]. The report indicates that anti-PD-1 treatment

may upregulate NTRK, which aberrantly activates the JAK-STAT signaling pathway, leading to an increase in inhibitory receptors on T cell surfaces, including PD-1, thereby promoting T cell exhaustion [27]. Consequently, while PD-1 inhibitors might enhance CAR-T function through depletion reduction, addressing how to counteract their adverse effects when combined ineffectively with CAR-T remains a critical research challenge. Given the complexity of the lymphoma tumor microenvironment, exploring whether alternative mechanisms regulate drug resistance within this context is essential.

Tumor-associated macrophages (TAMs) represent a crucial subset of immune cells within the tumor microenvironment. It has been reported that PD-1 inhibitors may affect the tumor microenvironment, and their mediated antibody dependent cellular phagocytosis (ADCP) can



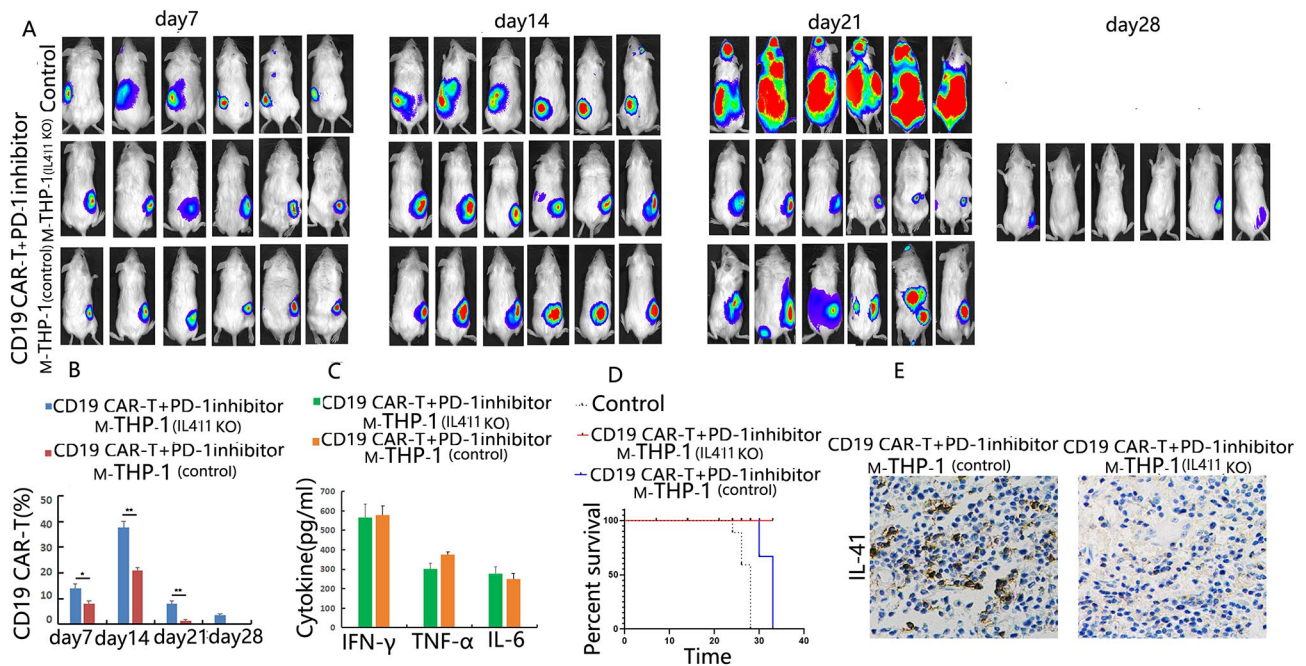


**Fig. 4** IL4I1 Inhibition in Macrophages Impedes CAR-T Treatment In Vivo. **(A)** The formation and progression of tumors in three groups of mice were monitored using bioluminescence imaging: the control group, the CAR-T+M-THP1 (IL4I1 KO)+PD-1 inhibitor group, and the CAR-T+M-THP1 (control)+PD-1 inhibitor group. Day 0 was established when engraftment was confirmed following the injection of Pfeiffer cells. **(B)** The percentage of CD19 CAR-T cells in the bone marrow over time was measured by flow cytometry. **(C)** Survival rates of the three mouse groups. Data in the bar graphs represent the mean  $\pm$  SD values from three experimental repeats ( $P < 0.05$ ; \*,  $P < 0.01$ ,  $n = 3$ )

trigger the immunosuppressive effect of macrophages in the tumor microenvironment [28]. Activation of macrophages via AIM2 during CAR-T therapy has been shown to release bioactive interleukin-1 $\beta$  (IL-1 $\beta$ ), significantly impairing CAR-T efficacy [7]. Our recent findings indicate that activated macrophages and associated oxidative stress could stimulate mesenchymal stem cells (MSCs) to secrete STC1, thus impacting CAR-T cytotoxicity [29]. Recent studies have showed that PD-1<sup>+</sup> TAMs predominantly exhibit an M2 polarization phenotype characterized by “tumor-suppressive” properties [30]. This suggests that PD-1 inhibitor therapy for DLBCL may modulate TAM immune remodeling. Therefore, it is necessary to find key immunomodulatory targets that affect TAMs to enhance the therapeutic effect of PD-1 inhibitors combined with CAR-T in DLBCL.

The researchers integrated 178,651 MNPs from 13 tissues in 41 datasets to generate the MNP Single-cell RNA Atlas (MNP-VERSE). In particular, the researchers focused on IL4I1<sup>+</sup>CD274(PD-L1)<sup>+</sup>IDO1<sup>+</sup> macrophages, which mature monocytes stimulated by IFN induced interferon- $\gamma$ (IFN- $\gamma$ ) and CD40/CD40L and aggregate around the tumor in a T-cell-dependent manner. IL4I1<sub>Mac</sub> exhibits immunosuppressive properties through tryptophan degradation and promotes the entry of regulatory T cells into tumors [16]. IL4I1 could be a promising immunotherapy target for selective modulation of TAMs

and stands as a novel macrophage-related prognostic biomarker in glioma [31]. ScRNA-seq analysis indicated that IL4I1 exhibits significant variability among different cell types within the tumor microenvironment, with its highest enrichment observed in macrophages. A positive correlation was found between various immune checkpoint genes and IL4I1 expression across most tumors. This suggests that IL4I1 may function as a promoter of cancer progression and serve as a prognostic indicator for patients. Elevated levels of IL4I1 are associated with tumor immunosuppression and may facilitate the invasion of tumor-associated macrophages [32]. Our results showed that IL4I1 expression was significantly higher in the tumor tissue of R/R DLBCL patients and correlated with poor prognosis. The positive correlation between IL4I1 and poor prognosis in patients underscores the importance of investigating IL4I1 as a potential therapeutic target.

Targeting metabolic pathways represents a promising strategy to enhance the efficacy of immunotherapy, particularly through the modulation of inhibitory immune cell metabolism, which can increase tumor lethality [33]. The activation of the aryl hydrocarbon receptor (AHR) pathway by metabolites derived from tryptophan decomposition may promote tumor progression while simultaneously inhibiting anti-tumor immunity [34]. IL4I1 functions as an amino acid oxidase expressed in

macrophages and activates the aryl hydrocarbon receptor (AHR) through tryptophan (Trp) recognition and indole metabolite production [35]. A study involving the use of the PD-1 monoclonal antibody nivolumab to treat advanced melanoma revealed an increase in the expression of IDO1 and IL4I1 [15]. IDO1 may be a root cause of the ineffectiveness of PD-1 inhibitors, and the combination of IDO1 inhibitors with PD-1 inhibitors has been explored in clinical trials [36, 37]. However, the outcomes of these trials have not conclusively demonstrated that IDO1 inhibitors can inhibit the activity of IL4I1 [38, 39]. Our experiment revealed that knockout of IL4I1 in macrophages enhanced the cytotoxicity of CD19 CAR-T therapy combined with a PD-1 inhibitor, both in vitro and in vivo. This suggests that reducing IL4I1 expression could potentially overcome resistance to PD-1 inhibitors when combined with CAR-T therapy. Our experiment also revealed that CD19 CAR-T therapy can activate the Trp-Kyn pathway by immunomodulatory roles of TAMs, which may contribute to drug resistance when combined with PD-1 inhibitors for DLBCL treatment. These findings emphasize the significance of targeting IL4I1 to improve the efficacy of combination therapies in the treatment of DLBCL. This further emphasizes the complex interactions within the tumor microenvironment and the need for a comprehensive understanding of the mechanisms involved in resistance to combination therapies.

Transcriptomic and metabolomic correlation analyses showed that AA-PGE2 metabolism passway were downregulated in control group than IL4I1 KO group. Therefore, whether IL4I1 improves the tumor microenvironment affected by macrophages by affecting AA-PGE2 lipid metabolism is also the key to our future exploration. At the same time, whether the elimination of IL4I1 in M-THP1 affects the polarization level of TAMs and whether it can reveal the internal relationship between metabolic pattern and phenotypic state is also the key for further exploration.

In conclusion, this study demonstrates the notable impact of macrophages in impeding the effectiveness of CAR-T cells when combined with PD-1 inhibitors. It also presents evidence implicating the IL-4I1 gene in mediating inhibitory mechanisms. While further investigation is warranted to elucidate the precise molecular interactions, the findings presented hold promising clinical implications for combating drug resistance in cancer therapy.

### Supplementary Information

The online version contains supplementary material available at <https://doi.org/10.1186/s12967-024-06028-3>.

Supplementary Material 1

Supplementary Material 2  
 Supplementary Material 3  
 Supplementary Material 4  
 Supplementary Material 5  
 Supplementary Material 6  
 Supplementary Material 7  
 Supplementary Material 8  
 Supplementary Material 9  
 Supplementary Material 10  
 Supplementary Material 11  
 Supplementary Material 12  
 Supplementary Material 13  
 Supplementary Material 14  
 Supplementary Material 15  
 Supplementary Material 16  
 Supplementary Material 17  
 Supplementary Material 18  
 Supplementary Material 19  
 Supplementary Material 20  
 Supplementary Material 21  
 Supplementary Material 22  
 Supplementary Material 23  
 Supplementary Material 24

### Acknowledgements

We appreciate the patients' assistance and cooperation as part of their involvement in the study. Also, we appreciate Tianjin First Central Hospital's support of our research. The entire laboratory staff of Tianjin First Central Hospital's Department of Hematology provided invaluable contributions to this research. We sincerely appreciate the cooperation and help provided by the Tianjin Medical University Animal Care and Use Committee. Particular thanks to Prof. Zhao for his helpful criticism of our study.

### Author contributions

Rui Zhang, Conceptualization, Formal analysis, Writing - Review and editing; Yi Zhang, Formal analysis; Hairong Xiao, Methodology; Qingxi Liu, Data curation; Mingfeng Zhao, Resources, Supervision, Conceptualization.

### Funding

This work was supported by grants from the General Project of the National Natural Science Foundation of China (81970180 to MZ), the Science and Technology Project of Tianjin Municipal Health Committee (TJWJ2022QN030 to MZ), the Key projects of Tianjin Applied Basic Research and Multi-Investment Fund (21JCZDJC01240), the Science and Technology Project of Tianjin Municipal Health Committee (TJWJ2022XK018 to MZ), and the Key Science and Technology Support Project of Tianjin Science and Technology Bureau (20YFZCSY00800 to MZ), as well as Tianjin Key Medical Discipline (Specialty) Construction Project (TJYXZDXK-056B).

### Data availability

All data generated or analyzed during this study are included in this published article.

## Declarations

### Ethics approval and consent to participate

Informed consent was provided with lymphoma and healthy donors agreed to participate in this experiment within a clinical trial. Ethics approval was provided at the Department of Hematology at Tianjin First Central Hospital (Tianjin, China) (ChiCTR-ONN-16009862; Tianjin First Central Hospital Medical Ethics Committee).

### Competing interest

The authors declared no potential conflicts of interest concerning the research, authorship, and/or publication of this article.

Received: 25 September 2024 / Accepted: 23 December 2024

Published online: 22 January 2025

## References

1. Coiffier B, Lepage E, Briere J, et al. CHOP chemotherapy plus rituximab compared with CHOP alone in elderly patients with diffuse large-B-cell lymphoma. *N Engl J Med*. 2002;346:235–42.
2. Taylor RB, Paolo FC. A paradox of choice: sequencing therapy in relapsed/refractory diffuse large B-cell lymphoma. *Blood Rev*. 2024;63:101140.
3. Schuster SJ, Bishop MR, Tam CS, et al. Tisagenlecleucel in adult relapsed or refractory diffuse large B-Cell lymphoma. *N Engl J Med*. 2019;380(1):45–56.
4. Rawan GF, Sae BL, Michael DJ, et al. Baseline serum inflammatory proteins predict poor CAR T outcomes in diffuse large B-cell lymphoma. *Blood Cancer Discov*. 2024;5(2):106–13.
5. Karen TM, Stephan AG, Shannon LM, et al. Tisagenlecleucel immunogenicity in relapsed/refractory acute lymphoblastic leukemia and diffuse large B-cell lymphoma. *Blood Adv*. 2021;5(23):4980–91.
6. Min Liu G, Bertolazzi S, Sridhar, et al. Spatially-resolved transcriptomics reveal macrophage heterogeneity and prognostic significance in diffuse large B-cell lymphoma. *Nat Commun*. 2024;8(1):2113.
7. Liu D, Xu X, Dai Y, et al. Blockade of AIM2 inflammasome or  $\alpha$  1-AR ameliorates IL-1  $\beta$  release and macrophage-mediated immunosuppression induced by CAR-T treatment. *J Immunother Cancer*. 2021;9(1):e001466.
8. Chong EA, Melenhorst JJ, Lacey SF, et al. PD-1 blockade modulates chimeric antigen receptor (CAR)-modified T cells: refueling the CAR. *Blood*. 2017;129:1039–41.
9. Su S, Zhao J, Xing Y, et al. Immune Checkpoint Inhibition overcomes ADCP-Induced Immunosuppression by macrophages. *Cell*. 2018;175:442–e5723.
10. Hui Liu W, Lei C, Zhang, et al. CD19-specific CAR T cells that Express a PD-1/CD28 chimeric switch-receptor are effective in patients with PD-L1-positive B-Cell lymphoma. *Clin Cancer Res*. 2021;27(2):473–84.
11. Qian LX, Feng ZY, Kaimin, Li, et al. A novel dominant-negative PD-1 armored anti-CD19 CAR T cell is safe and effective against refractory/relapsed B cell lymphoma. *Transl Oncol*. 2021;14(7):101085.
12. Cao Y, Lu W, Sun R, et al. Anti-CD19 Chimeric Antigen Receptor T Cells in Combination with Nivolumab are safe and effective against Relapsed/Refractory B-Cell non-hodgkin Lymphoma. *Front Oncol*. 2019;9:767.
13. Xue B, Luo X, Liu Y et al. CAR T-Cell Therapy Combined with PD-1 Inhibitors Significantly Improve the Efficacy and Prognosis of r/r DLBCL with TP53 Alterations. *Blood*. 2023, ASH 142 (Supplement 1): 3515.
14. De Matteis S, Casadei B, Lolli G, et al. Case report: Senescence as mechanism of resistance to Pembrolizumab in a lymphoma patient who failed CD19-Targeted CAR-T cell therapy. *Front Immunol*. 2022;13:994731.
15. Rahul Banerjee RC, Lynch Q, Wu, et al. A phase 2 study of Nivolumab for Relapsed/Refractory multiple myeloma or Non-hodgkin Lymphoma following CAR-T therapy. *ASH Blood*. 2023;142(Supplement 1):3509.
16. Zhao H, Teng Y, Hao W, et al. Single-cell analysis revealed that IL411 promoted ovarian cancer progression. *J Translational Med*. 2021;19:454.
17. Sadik A, Somarrivas Patterson LF, Öztürk S, et al. IL411 is a metabolic Immune checkpoint that activates the AHR and promotes Tumor Progression. *Cell*. 2020;182:1252–e7034.
18. Chouery F, Singh S, Sircar A et al. Integration of Metabolomics and Gene expression profiling elucidates IL411 as Modulator of Ibrutinib Resistance in ABC-Diffuse large B cell Lymphoma. *Cancers*. 2021;13(9):2146.
19. Taylor A, Harker JA, Chanthong K, et al. Glycogen synthase kinase 3 inactivation drives T-bet-mediated downregulation of co-receptor PD-1 to enhance CD8(+) cytolytic T cell responses. *Immunity*. 2016;44:274–86.
20. Zhang R, Wang N, Zhang LN, et al. Knockout of DNMT1 and DNMT3a promotes the angiogenesis of human mesenchymal stem cells leading to arterial specific differentiation. *Stem Cells*. 2016;34:1273–83.
21. Gargaro M, Scalisi G, Manni G, et al. Indoleamine 2,3-dioxygenase 1 activation in mature cDC1 promotes tolerogenic education of inflammatory cDC2 via metabolic communication. *Immunity*. 2022;55:1032–e5014.
22. Zhang YJ, Yang YHJ, et al. Non-viral, specifically targeted CAR-T cells achieve high safety and efficacy in B-NHL. *Nature*. 2022;609(7926):369–74.
23. Zhang Y, Li J, Lou X, et al. A prospective investigation of Bispecific CD19/22 CAR T cell therapy in patients with relapsed or refractory B cell Non-hodgkin Lymphoma. *Front Oncol*. 2021;11:664421.
24. Fraietta JA, et al. Ibrutinib enhances chimeric antigen receptor T-cell engraftment and efficacy in leukemia. *Blood*. 2016;127:1117–27.
25. Yoon DH, Osborn MJ, Tolar J, et al. Incorporation of immune checkpoint blockade into chimeric antigen receptor T cells (CAR-Ts): combination or built-in CAR-T. *Int J Mol Sci*. 2018;19:e340.
26. Elise A, Chong Cécile, Alanio J, Svoboda, et al. Pembrolizumab for B-cell lymphomas relapsing after or refractory to CD19-directed CAR T-cell therapy. *Blood*. 2022;139(7):1026–38.
27. Jessica M, Konen B, Leticia Rodriguez, Jared J, Fradette, et al. Ntrk1 promotes resistance to PD-1 checkpoint blockade in Mesenchymal Kras/p53 mutant Lung Cancer. *Cancers*. 2019;11(4):462.
28. Su S, Zhao J, Xing Y, et al. Immune Checkpoint Inhibition overcomes ADCP-Induced Immunosuppression by macrophages. *Cell*. 2018;175(2):442–e45723.
29. Zhang R, Liu Q, Zhou S, He H, Zhao M, Ma W. Mesenchymal stem cell suppresses the efficacy of CAR-T toward killing lymphoma cells by modulating the microenvironment through stanniocalcin-1. *Elife*. 2023;12:e82934.
30. Yavuz BG, Gunaydin G, Emre Gedik M, et al. Cancer associated fibroblasts sculpt tumour microenvironment by recruiting monocytes and inducing immunosuppressive PD-1 + TAMs. *Sci Rep*. 2019;9(1):3172.
31. IL41. 1 in M2-like macrophage promotes glioma progression and is a promising target for immunotherapy. *Front Immunol* 2024;14:1338244.
32. Pan-cancer analysis of. Prognostic and immunological role of IL411 in human tumors: a bulk omics research and single cell sequencing validation. *Discov Oncol*. 2024;15(1):139.
33. Reinfeld BI, Madden MZ, Wolf MM, et al. Cell-programmed nutrient partitioning in the tumor microenvironment. *Nature*. 2021;593(7858):282–8.
34. Cristina Gutiérrez-Vázquez and, Francisco J, Quintana. Regulation of the Immune response by the Aryl Hydrocarbon receptor. *Immunity*. 2018;48(1):19–33.
35. Molinier-Frenkel V, Prévost-Blondel A, Castellano F. The IL411 Enzyme: A New Player in the Immunosuppressive Tumor Microenvironment. *Cells*, 2019; 8.
36. Duan Z, Zhang S, Liang H, et al. Amyloid  $\beta$  neurotoxicity is IDO1-Kyn-AhR dependent and blocked by IDO1 inhibitor. *Signal Transduct Target Therapy*. 2020;5:96.
37. Xu M, Zhu F, Yin Q et al. Serum Response Factor-Regulated IDO1/Kyn-AhR Pathway Promotes Tumorigenesis of Oral Squamous Cell Carcinoma. *Cancers*. 2023; 15.
38. Wang Y, Li CM, Han R, et al. PCC0208009, an indirect IDO1 inhibitor, alleviates neuropathic pain and co-morbidities by regulating synaptic plasticity of ACC and amygdala. *Biochem Pharmacol*. 2020;177:113926.
39. Ladomersky E, Zhai L, Lauing KL, et al. Advanced Age increases Immunosuppression in the brain and decreases immunotherapeutic efficacy in subjects with Glioblastoma. *Clin cancer Research: Official J Am Association Cancer Res*. 2020;26:5232–45.

## Publisher's note

Springer Nature remains neutral with regard to jurisdictional claims in published maps and institutional affiliations.